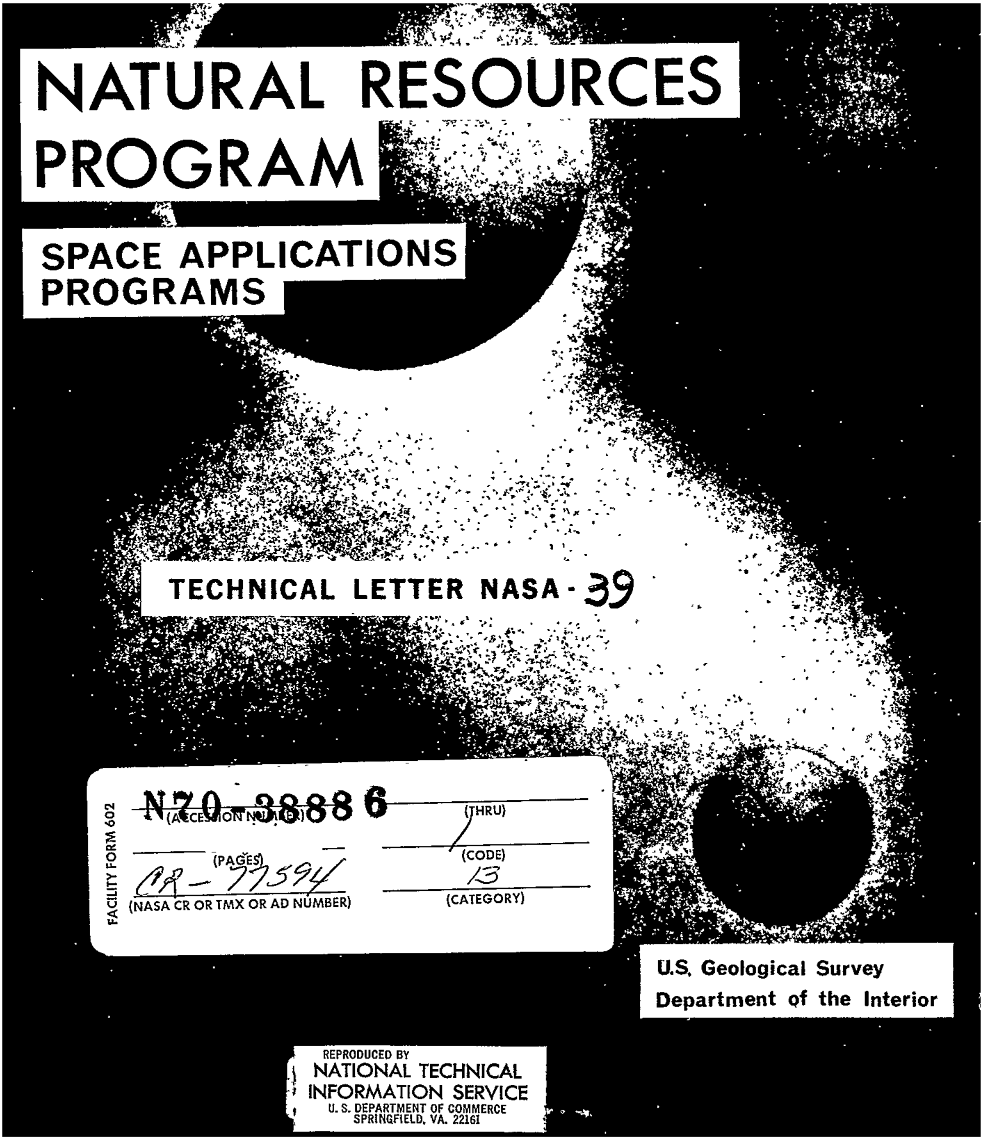

NATURAL RESOURCES PROGRAM

SPACE APPLICATIONS PROGRAMS

TECHNICAL LETTER NASA-39

U.S. Geological Survey
Department of the Interior

UNITED STATES
DEPARTMENT OF THE INTERIOR
GEOLOGICAL SURVEY
WASHINGTON, D.C. 20242

Technical Letter
NASA-39
August 1966

Dr. Peter C. Badgley
Chief, Natural Resources Program
Office of Space Science and Applications
Code SAR, NASA Headquarters
Washington, D.C. 20546

Dear Peter:

Transmitted herewith are 2 copies of:

TECHNICAL LETTER NASA-39

INTERPRETATION OF ULTRAVIOLET IMAGERY OF THE METEOR CRATER, SALTON SEA AND ARIZONA SEDIMENTARY TEST SITES (MISSION 18, JANUARY 1966)*

by

William R. Hemphill**

Sincerely yours,

William A. Fischer
Research Coordinator
Earth Orbiter Program

*Work performed under NASA Contract No. R-146-09-020-006
**U.S. Geological Survey, Washington, D.C.

UNITED STATES
DEPARTMENT OF THE INTERIOR
GEOLOGICAL SURVEY

TECHNICAL LETTER NASA-39

INTERPRETATION OF ULTRAVIOLET IMAGERY OF THE METEOR CRATER, SALTON SEA AND ARIZONA SEDIMENTARY TEST SITES (MISSION 18, JANUARY 1966)*

by

William R. Hemphill**

August 1966

These data are preliminary and should not be quoted without permission

Prepared by the Geological Survey for the National Aeronautics and Space Administration (NASA)

*Work performed under NASA Contract No. R-146-09-020-006
**U.S. Geological Survey, Washington, D.C.

Photo copies of illustrations are available for viewing at the following places:

Author(s); Discipline Coordinators; NASA Data Bank (Houston); Remote Sensing Evaluation and Coordination Staff (RESECS) and the U.S. Geological Survey Libraries (Denver, Menlo, Washington).

CONTENTS

ILLUSTRATIONS

10. Ultraviolet imagery of the Kaibab Limestone in the Came Springs area taken on January 8 and 9.

11. Ultraviolet imagery of part of the Cane Springs area showing the northeast trending fault in the Kaibab Limestone.

12. Cane Springs area.

    a. Ultraviolet imagery showing banded appearance of basalt lava and underlying older alluvium of Tertiary age.

    b. Conventional air photograph of the same area.

13. Ultraviolet imagery taken from an altitude of 5000 feet over the Imperial Valley near the northwestern shore of the Salton Sea.

14. Ultraviolet imagery taken from an altitude of 15,000 feet near the south shore of the Salton Sea.

15. Ultraviolet imagery along the southeastern shore of the Salton Sea.

APPENDIX

Appendix A. Plot showing variation in density of negative slate 354 of Meteor Crater, Arizona.

INTRODUCTION

The aircraft phase of the ultraviolet program is designed to produce ultraviolet imagery of geologic and terrain features for identification and direct comparison with imagery obtained with other sensors operating at longer wavelengths. The instrumentation consists of an optical-mechanical line scanner (fig. 1) mounted in NASA's multi-sensor equipped aircraft, a Convair 240. This aircraft is operated by the Flight Research Projects Branch, Manned Spacecraft Center in Houston. The scanner has since been modified and equipped with an ultraviolet sensitive photomultiplier detector featuring an S-11 photocathode; a Corning 7-60 filter limits the spectral response of the system to wavelengths shorter than 4050Å (fig. 2). The system is a so-called passive imaging system which uses the sun as a source of ultraviolet energy.

To date, reasonably satisfactory imagery has been obtained over the following NASA test sites: Pisgah Crater, Meteor Crater, Sedimentary test site, Twin Buttes, and the Salton Sea (fig. 3). The Pisgah Crater imagery has been discussed in another report (Hemphill, et al, 1965).

Imagery of the Twin Buttes was obtained in Mission 18 last January and is to be sent for evaluation to the cooperating investigator for this area, John Cooper, U.S. Geological Survey, Denver. This report discusses imagery obtained on Mission 18 of Meteor Crater, the Sedimentary test site, and the Salton Sea.

METEOR CRATER (Test site 28)

Seven flights were made over the crater between 0952 and 1039 hours on January 8, 1966. Altitude above terrain was 3500 feet for all flights. According to the Mission 18 flight log (1966), high, thin broken cloud cover made lighting conditions only somewhat better than marginal for color photography.

The first four runs (slate numbers 352,353, 354, and 355) produced imagery with the most contrast and shades of gray (fig. 4). The most highly reflective materials are unconsolidated debris around the margin of the crater and within the rim. Also highly reflective is the pale reddish brown sandstone near the base of the Moenkopi Formation of Triassic age (Shoemaker, 1959, p. 7); this sandstone contrasts markedly with overlying dark reddish brown siltstone as well as the underlying Kaibab Limestone of Permian age. Alluvium of dry stream washes also appears light in tone. The dark-toned thin line which appears in figures 4a and 4c below the rim of the east and southeast walls, marks the contact between vertical bedrock rim walls, and the unconsolidated talus slope beneath.

For comparison, figure 5 shows a conventional aerial photograph of the same area taken at about the same time. The area common to both the imagery and the photograph is outlined in figure 4c. Light-toned features are indicated throughout much of the conventional photograph including the area of Kaibab Limestone outcrop to the east of g.

In the ultraviolet imagery in figure 4c, however, the light-toned areas are generally limited to the sandstone outcrop. This suggests that this material, at least locally, has a relatively high reflectance in the ultraviolet, thus permitting the sandstone to be selectively imaged in the ultraviolet, while the outcrops of other rock types are reduced to below the noise level or are undistinguishab on the imagery in the absence of spectral contrast.

Figure 6 is an aerial photograph of the whole area shown in figure 4. However, because this photograph was taken in 1954 and not at the same time as the UV imagery, direct comparisons are limited.

On all the imagery shown in figure 4, changes in tonal contrast may be noted which appear to be independent of ultraviolet reflectance properties of ground features in the field of view (Appendix A). These tonal contrasts change abruptly at discrete scan lines in the imagery and may be due to random noise in the electronics of the system. However, at least some of the changes are due to adjustments in gain and other instrument controls by the operator during the overflight.

On figures 4a, 4c, and 4d, a marked change in contrast may be noted in the direction of flight directly over and just beyond the crater. This change could be due to operator manipulation of the flight deck controls during the overflight; it could also be due to operation of the instrument in the automatic gain control (AGC) mode.

The AGC is a device that permits a relatively constant output signal despite a comparatively wide variation in amplitude of the input signal. With a minimum of monitoring or human intervention, an AGC permits imaging of features with a wider range of reflectance properties than would be otherwise possible within the dynamic range of the system and recording film being used. The sensitivity of the system is automatically varied inversely with the amplitude of the input signal. In areas where ultraviolet reflectance is high, such as in the vicinity of the crater, the AGC may be, in effect, integrating the total ultraviolet reflectance from several features in the same or adjacent scan lines, thereby distorting the tonal density of images of individual features in and adjacent to the crater.

SEDIMENTARY TEST SITE (Test site 51)

Two runs were made over the sedimentary site (fig. 7), one at 1335 hours on January 8, 1966 and another at 10:30 on January 9, 1966 (Mission 18 flight log, 1966). Despite overcast sky and generally poor lighting conditions, imagery taken on January 8 shows more contrast and terrain detail than imagery taken the next day when the sky was clear. Figures 8 and 9 show imagery from two parts of the site taken on successive days, together with conventional air photographs taken at the same time as the imagery. Figure 8 shows the contact between Callville and Pakoon (?) Limestones of Carboniferous age on the north and surficial deposits of Quaternary and Recent age to the south. Figure 9 shows the Coconino Sandstone of Permian age and overlying surficial deposits. The preponderance of well defined detail, tonal contrast, and a more extensive gray scale in figures 8a and 9a, strongly suggests that instrument settings on January 8 were in a more closely optimum adjustment than on January 9 when weather and lighting conditions were improved. Adjustment of flight deck controls and configuration of the electronic data conditioning equipment in the scanner is apparently very critical and constitutes a more significant factor in obtaining high contrast imagery than weather conditions that prevailed at the time of the overflight.

Although the scanner apparently was "peaked" for near maximum performance during the January 8 overflight, this created a problem in some areas where ultraviolet reflectance was high, as for example, the Kaibab Limestone as shown in figure 10.

Detail to the west of the Kaibab Limestone outcrop, figure 10a, is obscured, probably as a direct result of the integrating effect of the AGC circuitry described above in the discussion of the Meteor Crater imagery. This was not a problem in the low contrast imagery taken on January 9 (fig. 10b).

The northeast trending fault in the Kaibab Limestone shows more clearly in the low contrast imagery (fig. 11b). However, this is believed to be a coincidence due to the fact that the west facing fault scarp has a more pronounced shadow in the January 9 imagery becuase this imagery was illuminated by a morning sun. Shadows were not pronounced on January 8 because of the overcast sky (fig. 11a).

In figure 12a, a dark toned basalt and underlying dark and light-toned beds of older Tertiary alluvium in the southern part of the site, present a pronounced banded appearance on the ultraviolet imagery. According to Lintz, et al, (1965), the Tertiary alluvial deposits are composed of pebbles, cobbles, and boulders of Pre-Cambrian metamorphic rocks and Paleozoic limestone. A conventional air photo taken at the same time is shown in figure 12b; alternating light and dark-toned patterns are less apparent on the photograph than on the imagery.

SALTON SEA (Site 27)

Fifteen runs were made over the Salton Sea area on January 11 and 12 at altitudes of 5000 and 15,000 feet above the terrain (Flight log, Mission 18, 1966). Figure 13 shows imagery taken at an altitude of 5000 feet over the Imperial Valley near the north-western shore of the sea. Despite the fact that the sky was cloudy, and the ultraviolet reception was described by the flight operator as "minimal", imagery shown in figure 13 is remarkably clear and free of noise. Tonal contrast is excellent.

Figure 14 shows a cultivated area near the shore of the Salton Sea. This imagery was taken from an altitude of 15,000 feet on January 12 when visibility was described as excellent (Flight log, Mission 18, 1966). Figure 15 is imagery of the southeastern shore of the Salton Sea, also from 15,000 feet. Both sets of imagery are remarkably clear for such extreme altitude; gray scale shows marked contrast between cultivated fields. Also clearly shown is the tonal variation apparently caused by turbidity where the Alamo River empties into the sea.

Agricultural significance of the Salton Sea imagery is being evaluated by A.B. Park and his associates at the Department of Agriculture.

CONCLUSIONS AND RECOMMENDATIONS

Image contrast of some features appear to be enhanced in the ultraviolet as compared to the same features on conventional aerial photographs. Also, the tonal contrast shown on the high altitude imagery of the Salton Sea, though a first attempt, was surprisingly good. Although significance of ultraviolet imagery (>3500A) in discriminating some geologic materials connot be evaluated on the basis of the limited tests completed to date; the program is continuing and repeated flights over these and other test sites should improve our ability to predict ultraviolet reflectivity and image tonal density in terms of specific geologic and terrain features, as well as atmosphere, altitude, and lighting limitations.

The test program to date suggests modifications in airborne operation of the ultraviolet line scanner. It is recommended that trial flights be made with and without the AGC circuitry in operation. Operation without the AGC should permit features to be imaged in terms of their own individual ultraviolet reflectance properties, and hopefully, would eliminate tonal anomalies in areas where ultraviolet reflectivity is high, such as at Meteor Crater. It is also recommended that necessary manipulation of gain, bias, and other settings on the flight deck control console be conducted before a run begins, and that the controls be "frozen", so to speak, during the run. Ideally, the same runs should be repeated with a variety of control settings. Of course, settings for each run would be recorded in the flight log.

Imagery obtained in future flights over the Meteor Crater test site could be improved if flight lines were oriented east-west instead of north-south. Two east-west flights were included on Mission 18; however, the ultraviolet imagery obtained was of too low contrast to be interpreted. Also, the run was of insufficient length to include several definitive outcrops of the Kaibab Limestone and Moenkopi Formation, and a well expressed fault to the east of the crater. At least one east-west flight, eight miles long centered on the crater, is suggested.

Laboratory studies in support of the aircraft program are planned and will include measurement of the distribution of spectral reflectance of selected test site rocks and surface materials, particularly those materials which appear to exhibit high reflectance in the ultraviolet, such as the sandstone near the base of the Moenkopi Formation in the Meteor Crater area.

The line scanner is a two channel or so-called "double ended" instrument. Plans to install a second photomultiplier on the channel not now being used have been temporarily slowed because of unforeseen technical problems during installation. A second channel is badly needed however, and fortunately it is expected that these installation problems will be overcome shortly.

The new photomultiplier will feature increased sensitivity at shorter wavelengths in the near ultraviolet. Also operation of a second channel will permit sumultaneous imaging at longer wavelengths in the visible for direct comparison with the ultraviolet imagery.

Interpretation would be facilitated because both ultraviolet and visible imagery would be recorded by the same system on the same medium, either film or tape. Use of conventional air photographs provided heretofore as a basis of comparison, is not satisfactory, mainly because of the great disparity between the 9x9 inch format and large scale of the photograph, and the small scale 35mm format of the imagery.

REFERENCES

Hemphill, W.R., Fischer, W.A., and Dornbach, J.E., 1965, Ultraviolet investigations for lunar missions; Proc. 11th Ann. Meeting Amer. Astronautical Soc., May 4-6, Chicago, Illinois.

Manned Spacecraft Center, 1966, Natural resources program remote sensing aircraft flight data summary report, NASA926, CV-240A, Mission 18 (unpub.); prepared by Flight Research Projects Branch Flight Crew Operations Directorate.

Shoemaker, E.M., 1959, Impact mechanics at Meteor Crater, Arizona; U.S. Geol. Survey open file report, Washington, D.C.

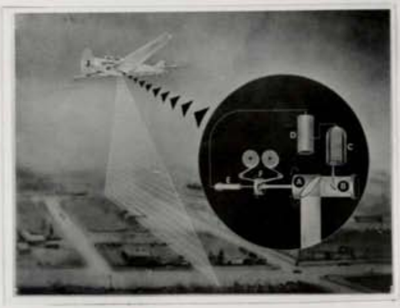

Figure 1 - Passive ultraviolet imaging system. Ultraviolet energy reflected from the earth's surface, is reflected by a rotating mirror, A, through a light-gathering optical system, B, and focused on an ultraviolet-sensitive photomultiplier, C. The photomultiplier output is amplified D, and modulates a glow-tube, E, whose line-scan motion is synchronized with the rotating mirror. Line scan image is recorded on photographic film, F. Lateral coverage is obtained by the rotating mirror; forward coverage is obtained by the forward travel of the aircraft.

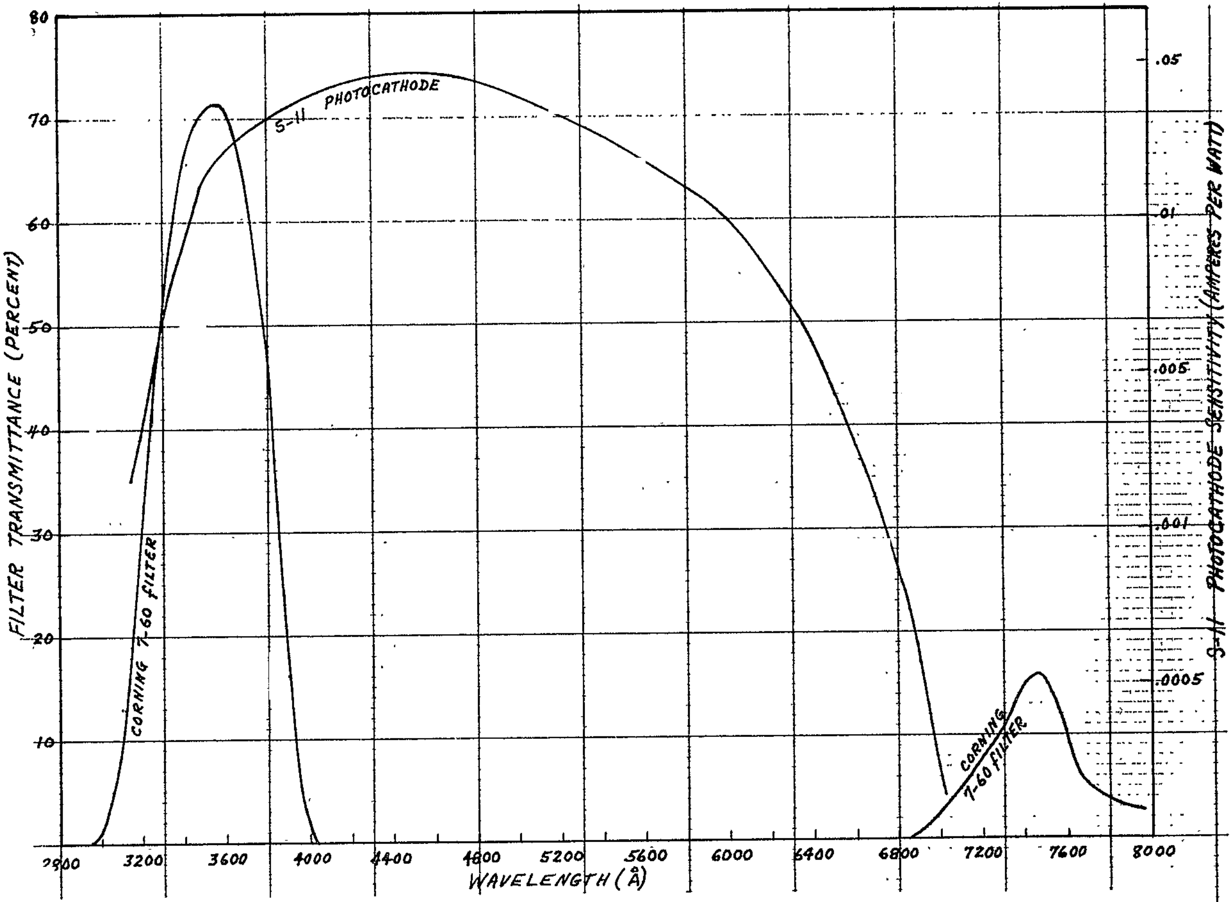

Figure 2 - Curves showing the relative sensitivity of the S-11 photocathode and transmittance of the Corning 7-60 filter.

Figure 3 - Index map showing location of NASA test sites.

Figure 4 - Ultraviolet imagery of Meteor Crater, Arizona taken from an altitude of 3500 feet above the terrain under marginal lighting conditions. Slate or run number 352 is shown in 4a; 353 in 4b, 354 in 4c, and 355 in 4d. All runs shown here were made during a 30-minute period during mid-morning of January 8, 1966. Arrows indicate the direction of flight. In 4c, features that apparently are highly reflective in the ultraviolet, and therefore contrast with surrounding features are indicated by letter symbols. Symbol a indicates a pale reddish brown sandstone near the base of the Moenkopi formation (Shoemaker, 1959); b notes light-toned alluvium deposited in dry stream beds; c indicates debris from the Coconino Sandstone and Kaibab Limestone that surrounds the outer margin of the crater; d shows talus within the rim; and e notes talings from exploratory shafts sunk in the floor of the crater. Area shown in the conventional aerial photograph in figure 5 is outlined in 4c.

Fig. 4a

Fig. 4b

Fig. 4c

Fig. 4d

15-B

FILM

Figure 5 - Conventional aerial photography taken at about the same time as the imagery shown in figure 4c. Area common to both is outlined in figure 4c. Contrast between the sandstone bed near the base of the Moenkopi formation(a) and the Kaibab limestone to the east is more pronounced on the ultraviolet imagery shown in figure 4c.

Figure 6 - Conventional aerial photograph of the entire area shown in Figure 4. Photograph was taken in 1954. Letter symbols are the same as described for Figure 4c.

Figure 7 - Geologic map of the sedimentary test site near Cane Springs in northwestern Arizona (Lintz and Brennan, 1965).

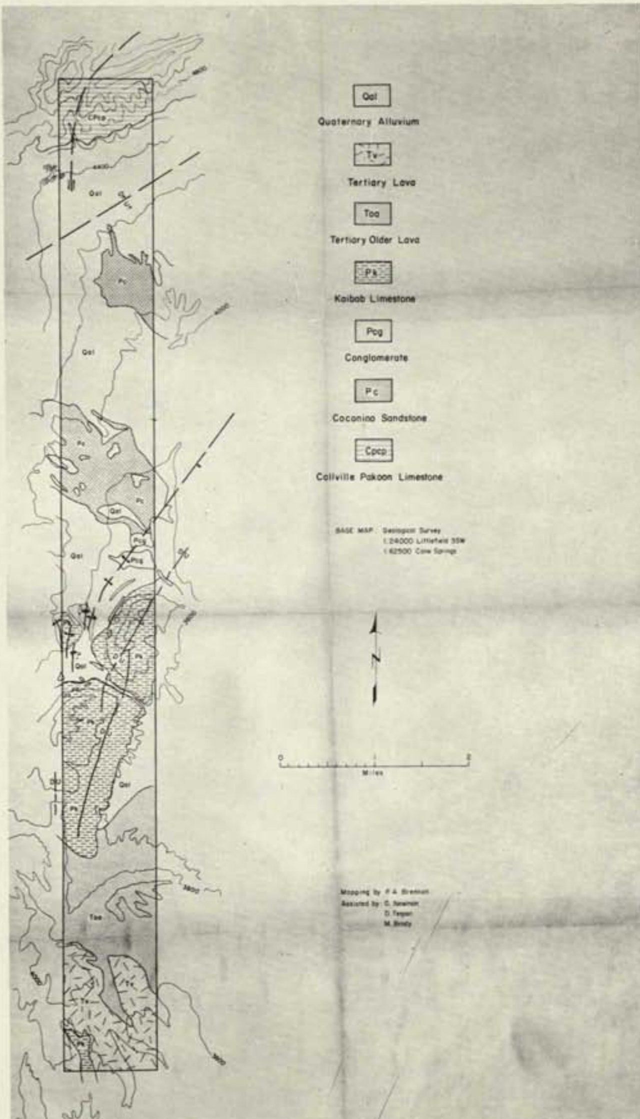

FIGURE-7

Sedimentary Fundamental Test Site
Cane Springs Arizona
Remote Sensing Project N.A.S.A.

18-A

Figure 8 - Ultraviolet imagery and a conventional aerial photograph taken simultaneously of part of the Cane Springs area showing the contact between Carboniferous limestones to the north and unconsolidated surface material to the south.

a. Ultraviolet imagery taken at about 13:35 on January 8.

b. Conventional air photograph taken at the same time as a.

c. Ultraviolet imagery taken at about 10:30 on January 9.

d. Conventional air photograph taken at the same time as c.

Despite poor lighting conditions on January 8, optimum control settings on the scanner permitted taking higher contrast imagery than on January 9 when lighting conditions had improved.

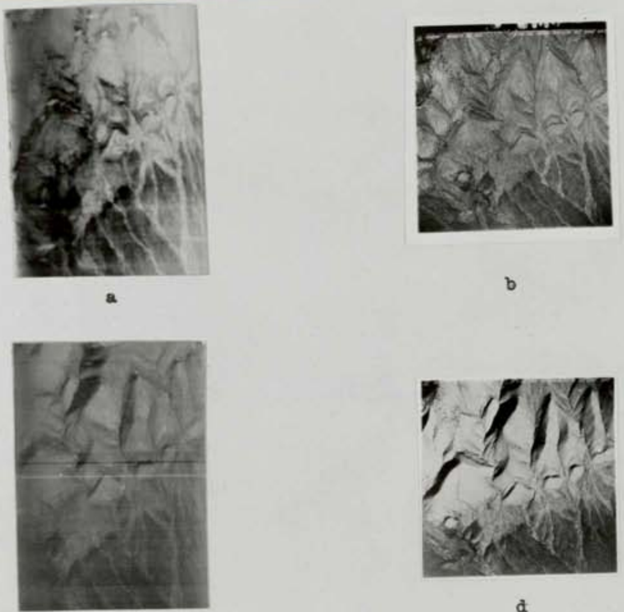

a b c d

Figure
-8-

CLASSIFICATION CANCELLED

BY AUTHORITY OF C. Donald Garrett

DATE Aug. 10, 1966

SIGNATURE Evelyn J. Chandler

FILM

Figure 9 - Ultraviolet imagery and conventional aerial photograph taken simultaneously of the Cane Springs area showing the Coconino Sandstone and overlying surficial deposits.

a. Ultraviolet imagery taken at about 13:35 on January 8.

b. Conventional air photograph taken at the same time as a.

c. Ultraviolet imagery taken at about 10:30 on January 9.

d. Conventional air photograph taken at the same time as c.

a

b

c

d

Figure
-9-

CLASSIFICATION CANCELLED
BY AUTHORITY OF C. Donald Garrett
DATE Aug 12, 1966
SIGNATURE Evelyn J. Chandler

Figure 10 - Ultraviolet imagery of the Kaibab Limestone in the Cane Springs area taken on January 8 (a), and on January 9 (b). Detail to the west of the Kaibab Limestone in 10a is obscure, apparently due to circuitry limitations in the scanner. In 10b, control settings of the scanner permitted imaging detail in this area; however, overall detail in this flight is low in contrast.

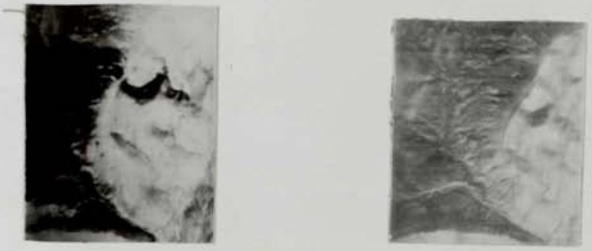

a b

Figure 10

CLASSIFICATION CANCELLED

BY AUTHORITY OF C. Donald Garrett

DATE Aug. 12, 1966

SIGNATURE Evelyn J Chandler

Figure 11 - Ultraviolet imagery of the Cane Springs area showing the northeast trending fault in the Kaibab Limestone.

a. Ultraviolet imagery taken at about 13:35 on January 8.

b. Ultraviolet imagery taken at about 10:30 on January 9.

Despite lower contrast, fault shows more clearly on January 9 imagery, because of a more favorable position of the sun.

a

b

Figure 11

22-A

CLASSIFICATION CANCELLED
BY AUTHORITY OF C. Donald Garrett
DATE Aug. 12, 1966
SIGNATURE Evelyn J. Chandler

Figure 12 - a. Ultraviolet imagery of the Cane Springs area showing banded appearance of basalt lava and underlying older alluvium of Tertiary age.

b. Conventional air photograph of the same area shown in a.

Both the imagery and the photograph were taken at about 13:35 on January 8.

1/

b

Figure -12-

Figure 13 - Ultraviolet imagery taken from an altitude of 5000 feet over the Imperial Valley near the northwestern shore of the Salton Sea. Tonal contrast between cultivated fields is considered to be excellent, despite poor lighting and atmospheric conditions.

Figure 13

CLASSIFICATION CANCELLED
BY AUTHORITY OF C. Donald Garrett
DATE Aug 10, 1966
SIGNATURE Evelyn J. Chandler

Figure 14 - Ultraviolet imagery taken from an altitude of 15,000 feet near the south shore of the Salton Sea. Despite extreme altitude, tonal contrast between cultivated fields is remarkably good.

Figure 14

CLASSIFICATION CANCELLED

BY AUTHORITY OF C. Donald Garrett

DATE Aug. 12, 1966

SIGNATURE Evelyn J. Chandler

Figure 15 - Ultraviolet imagery along the southeastern shore of the Salton Sea. Red Island, composed of rhyolite obsidian, is shown at a; Mullet Island at b; c marks a tonal variation which may be caused by turbidity where the Alamo River, d, empties into the Salton Sea. Unidentified areas that are highly reflective in the ultraviolet are shown at e and at f on the northern tip of Red Island.

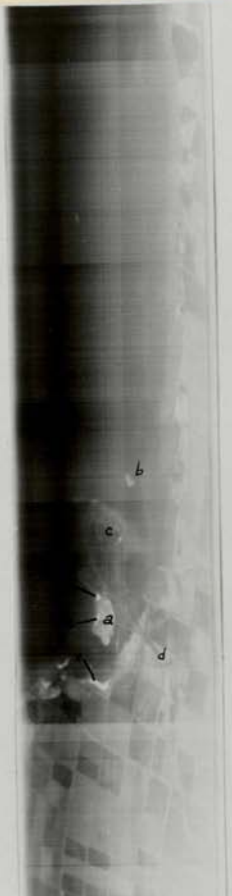

Figure 15

26-A

CLASSIFICATION CANCELLED
BY AUTHORITY OF C. Donald Garrett
DATE Aug 10, 1966
SIGNATURE Evelyn J. Chandler

Appendix A. Plot showing variation in density of negative of slate 354 of Meteor Crater, Arizona. Plot was obtained with a Joyce-Loebl microdensitometer (Model MK III CS) and a Technical Operations Laboratory Isodensitracer Model 565. Measurable variation in tonal contrast, apparently unrelated to geologic or terrain conditions, may be noted throughout the central part of the plot; cause of this variation is not known.

Abrupt change parallel to scan line south of the crater outline may be due to operator manipulation of flight-deck controls; it may also be due to operation of the instrument in the automatic gain control (AGC) mode.

Appendix A

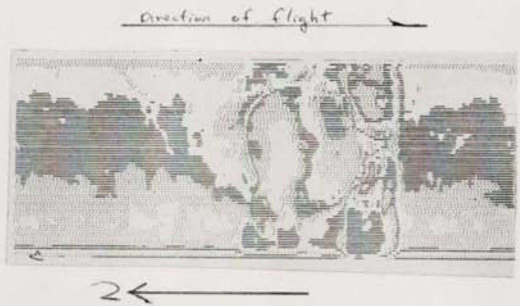

28